Infrared Spectroscopic Investigation of Photoionization-Induced Acidic C–H Bonds in Cyclic Ethers

ARTICLE *in* THE JOURNAL OF PHYSICAL CHEMISTRY A · MAY 2015

Impact Factor: 2.69 · DOI: 10.1021/acs.jpca.5b03406 · Source: PubMed

3 AUTHORS, INCLUDING:

Min Xie
Tohoku University
9 PUBLICATIONS **52** CITATIONS

SEE PROFILE

THE JOURNAL OF PHYSICAL CHEMISTRY A

Article

pubs.acs.org/JPCA

Infrared Spectroscopic Investigation of Photoionization-Induced Acidic C−H Bonds in Cyclic Ethers

Min Xie, Yoshiyuki Matsuda,* and Asuka Fujii*

Department of Chemistry, Graduate School of Science, Tohoku University, Aramaki-Aza-Aoba, Aoba-ku, Sendai, 980-8578 Miyagi, Japan

Supporting Information

ABSTRACT: Infrared (IR) predissociation spectroscopy based on vacuum-ultraviolet photoionization detection is performed for the neutral and cationic tetrahydrofuran (THF) and tetrahydropyran (THP). The CH bonds in neutral THF and THP are regarded as aprotic, even though the CH bonds are weakened by the negative hyperconjugation. After 118 nm photoionization, however, the negative hyperconjugation changes to the positive hyperconjugation and their CH bond acidities remarkably increase. In the IR spectrum of the THF cation, an intense band is observed at ca. 2700 cm^{-1}. This band is assigned to the antisymmetric stretch vibration of the two $C_\alpha H$ bonds next to the oxygen atom. The high intensity and low frequency of this band are due to the delocalization of the σ electrons of the two $C_\alpha H$ bonds to the singly occupied molecular orbital (SOMO) through the hyperconjugation. In the IR spectrum of the THP cation, on the other hand, the stretch bands of the $C_\alpha H$ bonds do not show obvious low-frequency shift and intensity enhancement, while the stretch band of the equatorial $C_\gamma H$ bond, at the *para*-position to the oxygen atom, appears at 2855 cm^{-1} with high intensity. This acidity enhancement of the equatorial $C_\gamma H$ bond is attributed to the mutiple hyperconjugation among the $C_\gamma H$ bond, two $C_\alpha C_\beta$ bonds, and SOMO of the oxygen atom. These results suggest that the difference of the hyperconjugation mechanism between the THF and THP cations arises from their preferable conformations.

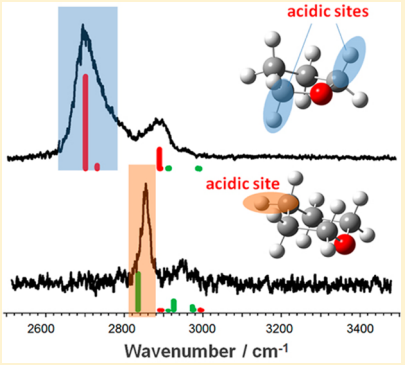

1. INTRODUCTION

Though neutral CH bonds are generally regarded as aprotic, remarkable enhancements of proton donor abilities of cationic CH bonds have recently been demonstrated.[1−12] Such enhancements of CH acidities would be one of key factors for proton-transfer reactions from CH in organic chemistry and environmental and interstellar processes because extra charge can often be involved in these processes. In the gas phase, various protonated products, which should be formed through proton transfer from CH bonds upon ionization, have been frequently observed in mass spectrometry.[1−4] With the optical spectroscopic approaches, intracluster proton-transfer reactions from CH bonds have been demonstrated in many cluster cations such as acetone dimer,[4] acetone−water,[5] and formamide−water.[6] Recently, infrared (IR) spectroscopy and theoretical reaction path search calculation have illustrated that proton transfer from a CH bond occurs without a barrier in the ionized trimethylamine dimer.[7] The photoelectron spectroscopy of the dimethyl ether dimer has also indicated barrierless proton transfer from CH in the cationic state.[8] These barrierless proton-transfer reactions from CH demonstrate that cationic CH can be highly acidic.

Evidence for enhancement of acidity of a cationic CH bond can be found in its stretch band observed by IR spectroscopy. Remarkable intensity enhancement of the CH stretch band has been reported in the toluene and *tert*-butyl cations.[9,10] Moreover, conformation dependence of the CH stretch frequency has recently been investigated for the methanol and diethyl ether cations.[11,12] The large variation of the stretch frequency and band intensity of the $C_\alpha H$ bond was found in the diethyl ether cation, and it was concluded that the acidity of the cationic CH bond highly depends on the internal rotational conformation of the ethyl group, which affects the hyperconjugation between the $C_\alpha H$ bond and the neighboring oxygen atom. The CH bond in the methanol cation also seems to undergo a large enhancement of the acidity similar to that of the diethyl ether cation. Because both of these molecules are rather flexible on internal rotation of the alkyl groups, interchange among isomers with the excess energy in the ionization process causes the difficulty in experimental study of the correlation between the hyperconjugation mechanism and conformation. Tetrahydrofuran (THF) and tetrahydropyran (THP) are cyclic ether molecules in which internal rotations of their alkyl groups are highly restricted. The conformational fluctuation is basically eliminated in these molecules, and we expect that the correlations between the hyperconjugation mechanism and molecular conformation can be clear.

To perform IR spectroscopic investigations of nonaromatic molecular cations in the gas phase, IR predissociation spectroscopy based on the vacuum-ultraviolet (VUV) photo-

Received: April 8, 2015
Revised: May 14, 2015
Published: May 15, 2015

DOI: 10.1021/acs.jpca.5b03406
J. Phys. Chem. A 2015, 119, 5668−5675

ionization detection has been shown to be a powerful tool.[13−15] In the present study, we apply this technique to the THF and THP cations to study their hyperconjugation mechanisms. Because THF and THP are cyclic ethers, which are prototypes of sugar rings seen in biomolecules, there have been a number of spectroscopic and theoretical studies on these two molecules.[16−29] However, to our knowledge, no spectroscopic study has been performed on the gas-phase acidity in their cationic state.

In this study, we carry out the IR spectroscopy of both the neutral and cationic of THF and THP based on the VUV-photoionization detection. In the neutral ground state of both the molecules, the negative hyperconjugations between the $C_\alpha H$ bonds and lone pair orbital in the oxygen atom weakens the $C_\alpha H$ bond strengths. In cationic THF, the positive hyperconjugation between the $C_\alpha H$ bonds and singly occupied molecular orbital (SOMO) is indicated by the IR spectral features. This positive hyperconjugation induces the remarkable enhancement of the acidities of the $C_\alpha H$ bonds. Thus, the hyperconjugation manner of THF switches from the negative hyperconjugation to the positive hyperconjugation through the ionization. In the THP cation of the chair-type conformer, the multiple hyperconjugations among the $C_\gamma H$, C_α-C_β, and SOMO are formed. Such correlations of the geometry and hyperconjugation mechanism are shown through comparisons of IR spectra and quantum chemical calculations.

2. METHODS

IR spectra of neutral and cations of THF and THP were recorded by IR predissociation spectroscopy based on the vacuum-ultraviolet photoionization detection. Details of the experimental setups have been described elsewhere,[15,30] and only a brief description is given here. Gaseous THF or THP seeded in the He carrier gas (at 3 atm total stagnation pressure) was expanded into the source chamber of a Wiley−McLaren type time-of-flight (TOF) mass spectrometer though a pulsed supersonic jet nozzle. The jet expansion was skimmed to form a molecular beam of 2 mm diameter, and the beam was introduced into the interaction region of the mass spectrometer. The tunable IR light and the VUV light at 118 nm were injected into the interaction region in the spatially counter-propagated manner. Ionized molecules were mass-selected and were detected by a microchannel plate (MCP). To measure an IR spectrum, the mass-selected ion intensity was monitored while the IR frequency was scanned. Whenever the IR light induces vibrational predissociation, the parent ion intensity is reduced and the fragment ion intensity is enhanced. In the present measurements, IR spectra of neutral and cationic THF and THP were obtained by monitoring their deprotonated fragment channels. The IR pulse was introduced ∼20 ns prior to the VUV ionization for spectroscopy of neutrals while the IR pulse injection was delayed by 20 ns to the ionization for spectroscopy of cations. The concentrations of THF and THP were controlled to prevent large cluster formation in the jet expansion.

The coherent VUV light (118 nm) was generated by tripling the third harmonic output (355 nm) of a Nd:YAG laser with a Xe−Ar mixture in the gas cell, which is attached directly at the vacuum chamber. The tunable IR light was generated by difference frequency generation (DFG) between the second harmonic output (532 nm) of a Nd:YAG laser and a dye laser output.

Geometry optimization, harmonic vibrational simulation, and nature bond orbital (NBO) analyses of THF and THP were performed with the Gaussian 03 and 09 packages.[31] For cations, the global reaction route mapping (GRRM) reaction path search calculation[32−34] combined with the Gaussian 03 or 09 package was performed at the PBE1PBE/6-31+G(d) level of theory. The vertically ionized structure was chosen as the starting point of the reaction path search. All the stable and transition structures obtained from the GRRM calculations were reoptimized by the ωB97X-D functional with the 6-311++G(3df,3pd) basis set. Their NBO analyses and IR spectral simulations were performed at the same level of theory.

Optimized structures are visualized by the GaussView 5 program.[35] The gas-phase acidities (ΔG_{acid}) of the C−H bond in the neutral and cationic molecules are defined by the Gibbs energy changes in the reactions $HA \rightarrow A^- + H^+$ and $HA^+ \rightarrow A^\bullet + H^+$, respectively. The energies of HA, A^-, HA^+, and $A^\bullet$ were calculated at the ωB97X-D/6-311++G(3df,3pd) level with the zero-point energy (ZPE) corrections. The gas-phase acidities were evaluated by the calculation at 298.15 K.

3. RESULTS AND DISCUSSION

3.1. Neutral THF. Neutral THF is a typical five-membered cyclic molecule and thus is not planar but puckered. Through the pseudorotation,[18,22] THF has two stable conformational isomers with C_2 and C_S symmetry (see Figure 1a). The energy difference between these two conformers has been estimated to be within 0.1 kcal/mol at several levels of theory.[21,22]

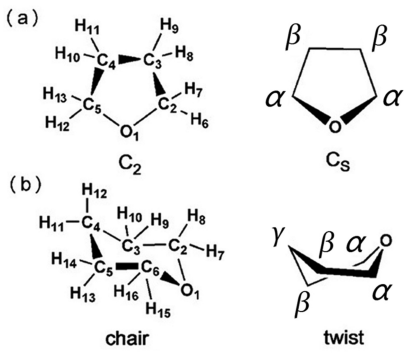

Figure 1. Molecular conformations (with atom labeling) of (a) THF and (b) THP.

The observed and calculated IR spectra of neutral THF are shown in Figure 2. In the observed spectrum (Figure 2a), two main features of CH stretching vibrations appear at ∼2862 and ∼2982 cm^{-1}. This jet-cooled spectrum is basically similar to the spectrum of liquid THF,[20,23] and no large changes of the CH stretching bands are found. Calculated IR spectra b and c of Figure 2 are simulated based on the optimized structures (C_2 and C_S, respectively). Their geometric parameters are listed in Table S1 of the Supporting Information. In the calculated spectra, the red sticks indicate the normal modes mainly composed by CH stretches of the carbon atoms at the α position (the α and β positions of the carbon atom are defined in Figure 1). The green sticks are the modes of CH stretches of the β carbon atoms. The yellow sticks are the modes involving both the $C_\alpha H$ and $C_\beta H$ stretches. Because of the similar features of the C_2 and C_S conformers in this frequency range and their small energy difference, it is difficult to determine the

DOI: 10.1021/acs.jpca.5b03406
J. Phys. Chem. A 2015, 119, 5668−5675

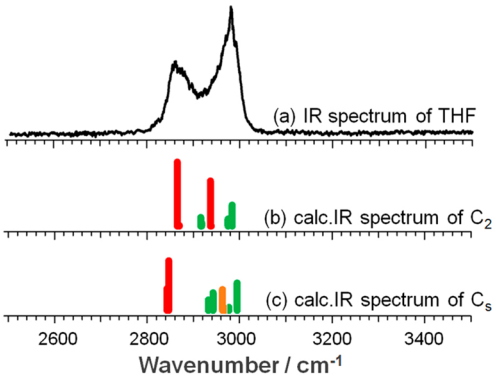

Figure 2. (a) Observed and (b,c) calculated IR spectra of neutral THF. In the calculated spectra, the red and green bands are assigned to the $C_\alpha H$ and $C_\beta H$ bonds, respectively. The yellow bands are attributed to the mixed vibration of the $C_\alpha H$ and $C_\beta H$ bonds. The calculated spectra are obtained by optimization at the ωB97X-D/6-311++G(3df,3pd) level with the scaling factor 0.95.

spectral carrier of the observed spectrum by comparison with the simulations.

The assignments of the vibrations of neutral THF have also been seen in the literature.[20,23,24] The normal-mode analyses based on the C_2 conformer have been performed.[20] Details of the assignments, which are simulated at the ωB97X-D/6-311++G(3df,3pd) level in this study, in the CH stretch region are described in Table S2 of the Supporting Information. Briefly, on the basis of these analyses, the peak at 2982 cm^{-1} is attributed to the $C_\beta H$ stretches. The $C_\beta H$ stretch frequencies have been estimated to be higher than those of $C_\alpha H$. The peak at 2862 cm^{-1} is assigned to the symmetric and antisymmetric $C_\alpha H$ stretches. The unresolved bands of the modes of CH stretches at the α and β positions are assigned to the absorption between the two main peaks. The present calculation of the C_2 conformer agrees well with the assignments presented in previous studies.

Both the previous assignments and present simulations show that the frequencies of the $C_\alpha H$ stretches tend to be lower than those of the $C_\beta H$ stretches. This trend of the CH stretch frequencies indicates the $C_\alpha H$ bond strength is lower than the $C_\beta H$ bond. This is due to the negative hyperconjugation[36−39] among the $C_\alpha H$ bonds and the nonbonding orbital of the oxygen atom. In this negative hyperconjugation, the nonbonding (lone pair, LP) electrons delocalize into the $C_\alpha H$ bonds. Table 1 shows the second-order perturbation energies, E(2), between the nonbonding orbital and the σ^* orbital (Lewis type NBO). They were calculated by the NBO analysis at the ωB97X-D/6-311++G(3df,3pd) level. E(2) reflects the magnitude of delocalization of electrons through (negative) hyperconjugation. In the table, only E(2) values larger than 1.0 kcal/mol are listed, and such strong interaction with LP are limited to the $C_\alpha H$ bonds. In the C_2 conformer, the E(2) values among the lone pair orbital and the σ^* orbitals of the $C_\alpha H$ bonds (C2−H7 and C5−H12) are nearly two times larger than those of the other two $C_\alpha H$ bonds(C2−H6 and C5−H13). In the case of the C_S conformer, the C2−H6 and C5−H12 bonds are axial and the C2−H7 and C5−H13 are equatorial. The E(2) values among the lone pair orbital and the σ^* orbitals of the axial CH bonds are higher than 5 kcal/mol, while those among the lone pair electrons and the σ^* orbitals of the equatorial CH bonds are lower than 2 kcal/mol. Thus, the interactions among the lone pair orbitals and the axial C−H bonds are much larger than those of the equatorial CH bonds. This is because the σ^* orbitals of the axial CH bonds better overlap with the lone pair orbitals. Hence, the axial $C_\alpha H$ bonds become weaker through the negative hyperconjugation in both of the C_2 and C_S conformers of THF.

Table 1. Second-Order Perturbation Energy E(2) (kcal/mol) for the Intramolecular Interactions in THF[a]

conformers		type of interaction	E(2)
neutral	C_2	LP → σ^*(C2−H7)	4.62
		LP → σ^*(C5−H12)	4.62
		LP → σ^*(C2−H6)	2.54
		LP → σ^*(C5−H13)	2.54
	C_S	LP → σ^*(C2−H6)	5.05
		LP → σ^*(C5−H12)	5.05
		LP → σ^*(C2−C3)	1.96
		LP → σ^*(C4−C5)	1.96
cation	C_2	σ(C2−H7) → LP*	22.47
		σ(C5−H12) → LP*	22.47
		σ(C2−H6) → LP*	8.09
		σ(C5−H13) → LP*	8.09

[a]Only the interactions larger than 1 kcal/mol are selected. In the neutral, the interactions with the oxygen lone pair (LP) electrons in the HOMO are shown. In the cation, the interactions with the electron in the SOMO are shown.

3.2. Cationic THF. Figure 3a shows the observed IR spectrum of cationic THF at the frequency range from 2500 to 3500 cm^{-1}. In the observed spectrum, an intense band is seen at 2700 cm^{-1} as well as a much weaker band at 2890 cm^{-1}. In this spectral range, only CH stretch bands are expected to appear for the THF cation. The band at 2890 cm^{-1} can be obviously assigned to a typical CH stretch band. On the other hand, the frequency of the intense band (2700 cm^{-1}) is out of the typical frequency range of CH stretches of alkyl groups (2850−3000 cm^{-1}). The high intensity and low frequency of this band would imply the characteristic property of the THF cation. Figure 3b presents the calculated infrared spectrum of the stable structure of the C_2 symmetry (depicted in the figure), which is the only stable conformer for the THF cation found through the GRRM reaction path search (there also exists an enantiomeirc isomer which has the same vibrational frequencies). The red and green sticks indicate the modes mainly

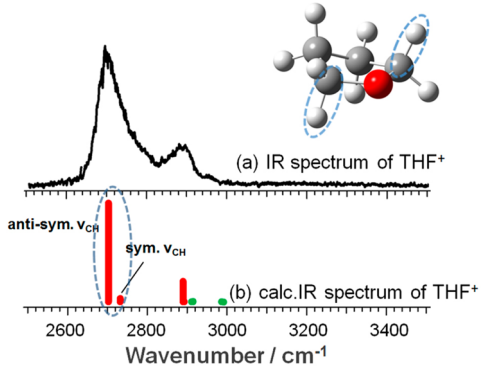

Figure 3. (a) Observed and (b) calculated IR spectra of cationic THF. In the calculated spectra, the red and green bands are assigned to $C_\alpha H$ and $C_\beta H$ bonds, respectively. The calculated spectra are obtained by optimization at the ωB97X-D/6-311++G(3df,3pd) level with the scaling factor 0.94.

DOI: 10.1021/acs.jpca.5b03406
J. Phys. Chem. A 2015, 119, 5668−5675

assigned to the $C_\alpha H$ and $C_\beta H$ stretches, respectively. The calculated spectrum well reproduces the observed features. The band at 2890 cm^{-1} is assigned to the antisymmetric and symmetric stretch vibration of the C2−H6 and C5−H13 stretches. The band at 2700 cm^{-1} is reproduced by the overlap of two bands: intense antisymmetric and weak symmetric modes of the C2−H7 and C5−H12 stretches.

The calculated energy diagram of the vertical ionization process of THF is shown in Figure 4. The ionization energy of

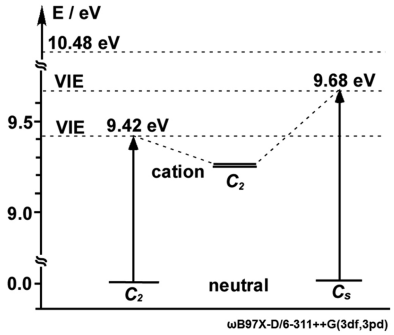

Figure 4. Energy diagram of the VUV one-photon ionization of THF from the neutral ground state. The stable structures and transition state of the cation were searched by the GRRM program at the UPBE1PBE/6-31+(d) level, and their relative energies (in kilocalories per mole) were obtained by reoptimization at the ωB97X-D/6-311++G(3df,3pd) level.

THF is about 9.7 eV.[17,18] Through the one-photon ionization at 118 nm (10.48 eV), one of the lone pair electrons of the oxygen atom is ejected. In the vertical ionization of both the neutral C_2 and C_S conformers, the produced ion can isomerize to the cationic C_2 structure without an energy barrier. These isomerization paths were simulated by the intrinsic reaction coordinate (IRC) calculations by use of the GRRM program package.

Table 1 lists E(2) for the interactions between the σ orbitals and the SOMO (LP*) of the oxygen atom in cationic THF. E(2) between SOMO and the σ orbitals of the C2−H7 and C5−H12 bonds is evaluated to be 22.5 kcal/mol. This large value originates from the delocalization of the σ electron of the C2−H7 and C5−H12 bonds to SOMO. This means that the negative hyperconjugation in the neutral is switched to the positive hyperconjugation upon the ionization. Moreover, the magnitude of the hyperconjugation in the cation is much larger than that in the neutral. The delocalization of the bonding σ electron causes the weakening of the CH bond strength and enlarges the partial positive charges of the hydrogen atoms. (The NBO charge distribution of cationic THF is shown in Figure S1 in the Supporting Information.) Thus, the high intensity of the observed band at 2700 cm^{-1} can be explained by the strong hyperconjugation among the C2−H7 and C5−H12 bonds and the SOMO.

The geometrical parameters of the neutral and cationic THF of the C_2 symmetry are shown in Table S1 of the Supporting Information. The most remarkable structural differences between the cation and neutral are the bond lengths of the C2−H7 and C5−H12 bonds. The cationic C2−H7 and C5−H12 bond lengths are 0.014 Å longer than those of the neutral C_2 conformer. These structural changes are caused by the hyperconjugation of these bonds with the SOMO.

Similar to the case of cationic diethylether (DEE) analyzed in our previous study,[12] the acidity of the $C_\alpha H$ bond in cationic THF remarkably increases upon the ionization because of the hyperconjugation. There is, however, differences between these two cases. Cationic DEE prefers the conformational structure in which only a single $C_\alpha H$ bond strongly interacts with the SOMO of the oxygen atom. On the other hand, the two $C_\alpha H$ bonds strongly hyperconjugate with SOMO in the THF cation. Therefore, both of these two hyperconjugated CH bonds should be acidic sites in cationic THF. The gas-phase acidity (ΔG_{acid}) of cationic THF is calculated to be 200.10 kcal/mol (at 278.15 K). This value decreases by 224.40 kcal/mol in comparison with that of neutral THF.

The full width at half-maximum (fwhm) of the low-frequency CH band in the IR spectrum of the THF cation is 73 cm^{-1}, which is 60 cm^{-1} less than that of the hyperconjugated CH band in the DEE cation. The simulated adiabatic and vertical ionization energies of THF are 9.27 and 9.42 eV at the ωB97X-D/6-311++G(3df,3pd) level, respectively, while those of DEE are 9.36 and 9.61 eV. Therefore, both ionized THF and DEE with the 118 nm light (10.5 eV) can have excess energies less than ∼1 eV. These excess energies can contribute to the broadening of the bandwidths. In the DEE cation, the magnitude of the hyperconjugation strongly depends on the internal rotation angle of the ethyl group, which changes the spatial overlap between the interacting orbitals, and the large bandwidth is mainly attributed to the excitation of the ethyl rotation.[12] On the other hand, in the THF cation, the internal rotation of the ethyl group is restricted by the cyclic structure, and this reduces the bandwidth relative to the DEE cation. In other words, the difference of the width indirectly evidences the large influence of the internal rotation to the hyperconjugation in the DEE cation. The bandwidth in the THF cation, however, seems rather large when we consider that the band originates only from the two CH stretches and that there is no isomer for the THF cation. In the vertical ionization of a neutral species, much energy is often deposited into the internal energy of the cation, reflecting structural differences between the neutral and cation. Figure 4 shows that both the neutral C_2 and C_S conformers have large internal energy after the ionization, and the produced cations are warm. Because of the low energy barrier of the pseudorotation, the magnitude of the hyperconjugations can be influenced by the large internal energy in the cations. Therefore, the width of the CH band is mainly attributed to the variation of the hyperconjugation due to the thermal excitation of the pseudorotation. This interpretation is essentially the same as that for the DEE cation, though the molecular geometry of THF is more rigid and the influence of the geometry fluctuation is more suppressed in the THF cation.

3.3. Neutral THP. THP is a six-membered heterocyclic saturated molecule. Six-membered cyclic molecules are well-known to have two main stable conformations of the chair and twist types.[27] Figure 1b shows the structure (with numbering of the atoms) of THP and its conformations. These conformers of neutral THP have been computationally simulated as the stable structures. The present theoretical calculations at the ωB97X-D/6-311++G(3df,3pd) level also confirm that these two conformers are stable. At this level, the chair conformer is 5.83 kcal/mol more stable than the twist conformer. Microwave spectroscopic study also has reported neutral THP favors the chair conformer.[40]

Figure 5a shows the observed and calculated IR spectra of neutral THP in the CH stretch region. Two main features of

DOI: 10.1021/acs.jpca.5b03406
J. Phys. Chem. A 2015, 119, 5668−5675

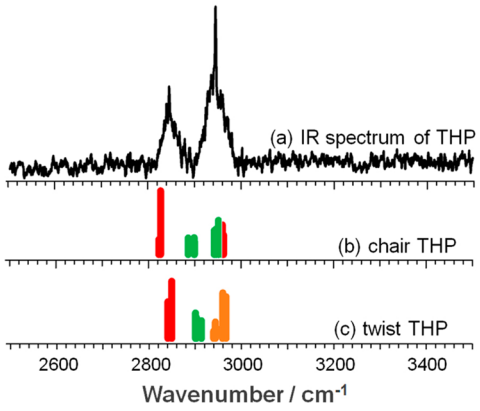

Figure 5. (a) Observed IR spectrum of neutral THP and (b, c) calculated IR spectra of the chair and twist conformers of neutral THP, respectively. In the calculated spectra, the red sticks indicate the modes assigned to the $C_\alpha H$ stretches. The green sticks indicate the $C_\beta H$ and $C_\gamma H$ stretch modes. The yellow sticks are the mixed stretch modes of all three types of the CH bonds ($C_\alpha H$, $C_\beta H$ and $C_\gamma H$). The calculated spectra are obtained by optimization at the ωB97X-D/6-311++G(3df,3pd) level with the scaling factor 0.95.

the CH stretching vibrations are observed at 2845 and 2945 cm^{-1}. The calculated spectra (spectra b and c in Figure 5) are based on the stable chair and twist conformers, respectively. The red sticks in the calculated spectra indicate the modes assigned to the $C_\alpha H$ stretches. The green sticks indicate the $C_\beta H$ and $C_\gamma H$ stretch modes. The yellow sticks are the mixed stretch modes of all three types of the CH bonds ($C_\alpha H$, $C_\beta H$, and $C_\gamma H$). Detailed assignments of the CH bands of THP are illustrated in Table S4 of the Supporting Information. The stretch frequencies of $C_\alpha H$ tend to be lower than those of the other CH bonds. This implies the the $C_\alpha H$ bond is weaker through the negative hyperconjugation than the other CH bonds, similar to the case of neutral THF.

Table 2 lists E(2) for the lone pair orbital of the oxygen atom and the σ^* orbitals of CH or CC bonds next to the oxygen atom in THP. Only E(2) values larger than 1.0 kcal/mol are shown in the table. In neutral THP, the lone pair orbital interacts with the σ^* orbitals of the C2−C3 and C5−C6 bonds as well as the axial $C_\alpha H$ bonds (C2−H8 and C6−H16). The energy differences between these two kinds of E(2) (hyperconjugations with the axial C−H and with the C−C bonds) are ∼1 kcal/mol. The E(2) values between the lone pair orbital and the σ^* orbitals of the equatorial $C_\alpha H$ bonds (C2−H7 and C6−H15) are smaller than 1.0 kcal/mol because of the poor spatial overlap between the orbitals. The hyperconjugation mechanisms and magnitudes are slightly different between THF and THP. These differences originate from their structural preferences which depend on the balance among the conformational factors such as steric repulsion and negative hyperconjugation.

3.4. Cationic THP. Figure 6a presents the observed IR spectrum of cationic THP. An intense band appears at 2855 cm^{-1}, and another band with much lower intensity is seen at 2952 cm^{-1}. The band at 2855 cm^{-1} seems to undergo an intensity enhancement similar to that of cationic THF, although its frequency is much higher than that of the band (2700 cm^{-1}) of cationic THF. Two structures depicted in Figure 6 are stable conformers of cationic THP. One is the chair conformer, and the other is the twist conformer. Similar to neutral THP, the chair conformer is simulated to be more stable by 5 kcal/mol than the twist conformer. In the calculated spectra shown in spectra b and c Figure 6, which are based on the chair and twist conformers, respectively, the red sticks indicate the modes assigned to the $C_\alpha H$ stretches. The green sticks indicate the $C_\beta H$ and $C_\gamma H$ stretch modes. The yellow sticks are the mixed CH stretch modes of all three types of the CH bonds ($C_\alpha H$, $C_\beta H$, and $C_\gamma H$). Because the calculated band frequencies of the two conformers are different from each

Table 2. Second-Order Perturbation Energy E(2) (kcal/mol) for the Intramolecular Interactions in THP[a]

conformers		type of interaction	E(2)
neutral	chair	LP → σ^*(C2−H8)	4.26
		LP → σ^*(C6−H16)	4.26
		LP → σ^*(C2−C3)	3.28
		LP → σ^*(C5−C6)	3.28
	twist	LP → σ^*(C2−H7)	5.06
		LP → σ^*(C5−C6)	4.07
		LP → σ^*(C6−H15)	3.42
		LP → σ^*(C2−C3)	2.02
cation	chair	σ(C2−C3) → LP*	19.46
		σ(C5−C6) → LP*	19.46
		σ(C2−H8) → LP*	3.24
		σ(C6−H16) → LP*	3.24
		σ(C4−H11) → σ^*(C2−C3)	2.53
		σ(C4−H11) → σ^*(C5−C6)	2.53
		σ(C2−H7) → LP*	1.70
		σ(C6−H15) → LP*	1.70
	twist	σ (C5−C6) → LP*	20.16
		σ (C2−H7) → LP*	16.58
		σ (C6−H15) → LP*	9.80
		σ (C2−H8) → LP*	3.95
		σ (C2−C3) → LP*	1.48
		σ(C4−H11) → σ^*(C5−C6)	1.75
		σ(C4−H11) → σ^*(C2−C3)	1.39

[a]Only the interactions larger than 1 kcal/mol are selected. In the neutral, the interactions with the oxygen lone pair (LP) electrons in the HOMO are shown. In the cation, the interactions with the electron in the SOMO are shown.

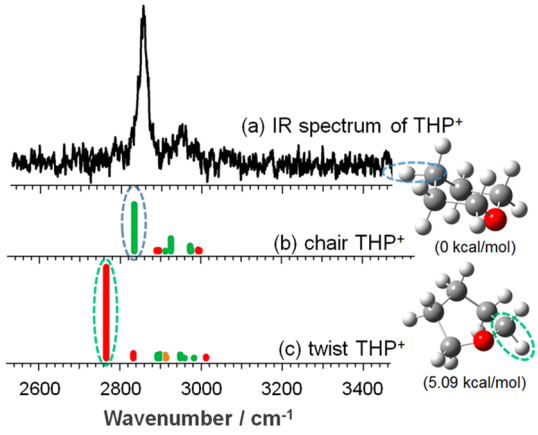

Figure 6. (a) Observed IR spectrum of cationic THP and (b,c) calculated IR spectra of the chair and twist conformers of cationic THP, respectively. The red sticks in the calculated spectra indicate the modes assigned to the $C_\alpha H$ stretches. The green sticks indicate the $C_\beta H$ and $C_\gamma H$ stretch modes. The yellow sticks are the mixed stretch modes of all three types of the CH bonds ($C_\alpha H$, $C_\beta H$, and $C_\gamma H$). The calculated spectra are obtained by optimization at the ωB97X-D/6-311++G(3df,3pd) level with the scaling factor 0.94.

DOI: 10.1021/acs.jpca.5b03406
J. Phys. Chem. A 2015, 119, 5668−5675

other, only one of them would be responsible for the observed spectrum. Although the calculated spectral patterns of both conformers are similar to each other, calculated spectrum (spectrum b in Figure 6) of the chair conformer seems to fit better with the observed one.

The energy diagram of the isomerization process following the ionization of THP is shown in Figure 7. After the vertical

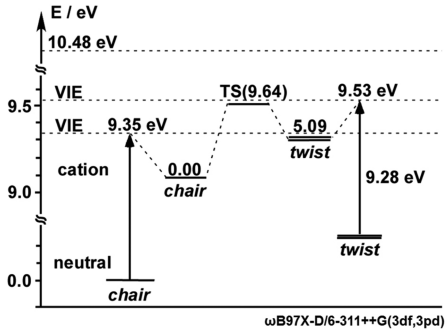

Figure 7. Energy diagram of the VUV one-photon ionization of THF from the neutral ground state. The stable structures and transition state of the cation were searched by the GRRM program at the UPBE1PBE/6-31+(d) level, and their relative energies (in kilocalories per mole) were obtained by reoptimization at the ωB97X-D/6-311++G(3df,3pd) level.

ionization of the neutral chair conformer, the molecular geometry changes to the cationic stable chair conformer without an energy barrier. Also in the vertical ionization of the twist conformer, the produced ion directly relaxes to the cationic twist conformer. The transition state between the cationic chair and twist conformers locates at 9.64 kcal/mol, which is the intermediate value between the vertically ionized structures of the two neutral stable conformers. Thus, the cationic chair conformer can energetically be formed through the ionization of both the neutral conformers. Because the energetics of the ionization also supports the production of the chair conformer, we therefore conclude that the chair conformer dominantly contributes to the observed IR spectrum. The band at 2855 cm^{-1} is assigned to the asymmetric stretching vibrations of the $C_\gamma H_2$ bond modes of the chair conformer.

The observed spectrum demonstrates that the $C_\gamma H$ stretch bands undergo the intensity enhancement in the THP cation, while the $C_\alpha H$ stretch band intensities are enhanced in the THF cation. The $C_\gamma H$ stretch band frequency of THP cation is within the typical alkyl CH stretch frequency range, although it is the lowest CH stretch band observed in cationic THP. On the other hand, the intense mode at 2766 cm^{-1} in the simulated spectrum of the twist conformer of the THP cation is attributed to the stretch mode of the $C_\alpha H$ (C2−H7) bond. We should note that the bond which is responsible for the intense CH stretch band in the simulation is different between the chair and twist conformers. This difference implies the hyperconjugation mechanism strongly correlates with the molecular geometries.

In Table 2, E(2) energies of the interactions between SOMO (LP*) and σ orbitals (Lewis type NBO) in the chair and twist cations are also listed. The geometric parameters simulated at the ωB97X-D/6-311++G(3df, 3pd) level are shown in Tables S3 and S4 of the Supporting Information. In the chair conformer, the E(2) energies between the σ orbitals of the two $C_\alpha C_\beta$ (C2−C3 and C5−C6) bonds and SOMO are the largest values at ca. 20 kcal/mol. These large E(2) energies are reflected by the elongation of the $C_\alpha C_\beta$ bonds in the cationic state (see the Supporting Information). The E(2) energies between the σ orbitals of the $C_\alpha H$ (C2−H8 and C6−H16) bonds and SOMO are 3.24 kcal/mol. These are much smaller than those (22.5 kcal/mol) in cationic THF. The C2−H8 and C6−H16 bonds of cationic chair THP are actually estimated to be shorter than those of the neutral. This is because the negative hyperconjugation (delocalization of the nonbonding electron to σ ($C_\alpha H$)) in the neutral state is more effective for the $C_\alpha H$ bond weakening than the positive hyperconjugation in the cation. On the other hand, the σ orbital of the C4−H11 bond interacts with the σ^* orbitals of the C2−C3 and C5−C6 bonds with E(2) at 2.53 kcal/mol, respectively. These interactions indicate that the σ electron of the C4−H11 bond delocalizes into these $C_\alpha C_\beta$ bonds through their hyperconjugation, while the $C_\alpha C_\beta$ bonds hyperconjugate also with the SOMO. These multiple hyperconjugations induce the elongation of the C4−H11 bond (increase by 0.008 Å) as well as the increase of the partial positive charge of the H11 atom. Thereby, the H11 atom has a larger positive charge at 0.283 au than those of the other H atoms (0.230−0.255 au). (The NBO charge distribution of cationic THP is seen in Figure S1 in the Supporting Information.)

This hyperconjugation mechanism accounts for the intensity enhancement of the $C_\gamma H$ stretch band of the chair conformer in the THP cation. Being the same as the positive hyperconjugation in cationic THF, the positive hyperconjugation (the delocalization of the σ electron of the $C_\gamma H$ bond) induces the acidity enhancement of the bond. However, the E(2) energies between the $C_\gamma H$ and $C_\alpha C_\beta$ bonds are smaller than those of the $C_\alpha H$ bond and SOMO in the THF cation. This difference appears as the smaller low-frequency shift of the $C_\gamma H$ stretch band of cationic THP than that of the $C_\alpha H$ bond of cationic THF.

Both the neutral and cation of THP prefer to form the similar chair-type structures. The SOMO dominantly hyperconjugates with the C_α-C_β bonds in cationic THP, while the lone pair orbital hyperconjugates with the C_α-H bonds in the neutral. The structural changes of the dihedral angles of C3−C2−O1−C6 and C6−O1−C2−H8 (see Table S3 of the Supporting Information) through the ionization enhance the magnitudes of overlaps of the σ orbitals of the C_α−C_β bonds and SOMO in the cationic state.

In the twist conformer of the THP cation, the C5−C6 and C2−H7 bonds show the largest E(2) energies with SOMO. These are also reflected by the elongation of these bonds. On the other hand, the E(2) between σ^*(C5−C6) and C4−H11 bond is only 1.39 kcal/mol. Therefore, the normal modes involving the C2−H7 stretch undergo the intensity enhancement, as seen in Figure 6c. These simulation results indicate the C2−H7 ($C_\alpha H$) bond is the acidic site in the twist conformer.

In the chair conformer of the THP cation, the acidity of the $C_\gamma H$ bond is largely enhanced by the multiple hyperconjugations among the $C_\gamma H$ bond, $C_\alpha C_\beta$ bond, and SOMO, while the $C_\alpha H$ bond becomes acidic in the twist conformer by the hyperconjugation directly with SOMO. The ΔG_{acid} value of the $C_\gamma H$ bond of the cationic chair conformer is calculated to be 210.80 kcal/mol (at 298.15 K). That of the $C_\alpha H$ bond of the twist conformer is 205.12 kcal/mol. They decrease 211.83 and 219.65 kcal/mol, respectively, compared with that of their neutrals. The hyperconjugation mechanism is different between the chair and twist conformers. The hyperconjugation

DOI: 10.1021/acs.jpca.5b03406
J. Phys. Chem. A 2015, 119, 5668−5675

mechanism correlates with the molecular geometries because spatial overlap between orbitals is a key factor in hyperconjugation. Hyperconjugation stabilizes the molecule while destabilization due to steric repulsion can compete with it. Preferred geometries of the molecule and their total stabilization energies are results of the balance between these factors. The difference of the hyperconjugation mechanism between cationic THF and THP can be explained by this balance. Thus, the acidic CH site in cations is also determined by their geometry preference coming from the balance among the energy factors.

4. CONCLUSIONS

The hyperconjugation mechanism in the neutrals and cations of THF and THP was investigated by the IR spectroscopy and theoretical calculations. The $C_\alpha H$ bonds in both the neutrals of THF and THP undergo negative hyperconjugation with the nonbonding orbital of the oxygen atom. In cationic THF, the positive hyperconjugation occurs between the $C_\alpha H$ bonds and SOMO, and the σ electron of $C_\alpha H$ delocalizes to the SOMO. Hence, the hyperconjugation manner in THF switches from the negative hyperconjugation to the positive hyperconjugation through the ionization. The positive hyperconjugation causes the obvious weakening of the $C_\alpha H$ bonds strength and the increase of the positive charge in the H atoms of the $C_\alpha H$ bonds, so that the acidity of the $C_\alpha H$ bonds is remarkably enhanced. In cationic THP, the multiple hyperconjugations among the SOMO, $C_\alpha-C_\beta$ bond, and $C_\gamma H$ bond induce the enhancement of the acidity of the $C_\gamma H$ bond. Thus, the hyperconjugation mechanism of cationic THF differs from that of cationic THP. This shows that the hyperconjugation mechanism depends on structural preference which comes from total balance among energy factors involving hyperconjugation.

Acidity enhancements of cationic OH and NH bonds have been known for various protic molecules. As seen in this study, positive hyperconjugation with the SOMO can increase acidities of cationic CH bonds, which are generally regarded as aprotic in the neutral state. The correlation between geometry and hyperconjugation mechanism, demonstrated for cationic THF and THP, would play an important role in many ion−molecule reactions in interstellar and atmospheric chemistry and chemical reactions accompanying charge fluctuations.

■ ASSOCIATED CONTENT

Supporting Information

Assignments of the CH bands of neutral THF and THP; geometrical parameters of the neutral and cationic isomers of THF and the chair and twist isomers of neutral and cationic THP; charge distribution of THF and THP. The Supporting Information is available free of charge on the ACS Publications website at DOI: 10.1021/acs.jpca.5b03406.

■ AUTHOR INFORMATION

Corresponding Authors

*E-mail: matsuda@m.tohoku.ac.jp. Fax: +81(0)22 795 6785. Tel: +81(0)22 795 6573.

*E-mail: asukafujii@m.tohoku.ac.jp. Fax: +81(0)22 795 6785. Tel: +81(0)22 795 6573.

Notes

The authors declare no competing financial interest.

■ ACKNOWLEDGMENTS

We thank Dr. T. Maeyama for his helpful discussions. M.X. appreciates the Guangzhou Elite Project for the Ph.D. scholarship. Y.M. acknowledges support from the Sumitomo Foundation and the Grant-in-Aid for Scientific Research (Project 26108504 on Innovative Area [2507]) from MEXT Japan. A.F. acknowledges the Grant-in-Aid for Scientific Research (Project 26288002) from JSPS.

■ REFERENCES

(1) Meot-Ner Mautner, M. The Ionic Hydrogen Bond. *Chem. Rev.* **2005**, *105*, 213−284.

(2) Garvey, J. F.; Peifer, W. R. Some Novel Ion−Molecule Chemistry within van der Waals Clusters. *Acc. Chem. Res.* **1991**, *24*, 48−54.

(3) Golan, A.; Bravaya, K. B.; Kudirka, R.; Kostko, O.; Leone, S. R.; Krylov, A. I.; Ahmed, M. Ionization of Dimethyluracil Dimers Leads to Facile Proton Transfer in the Absence of Hydrogen Bonds. *Nat. Chem.* **2012**, *4*, 323−329.

(4) Matsuda, Y.; Hoki, K.; Maeda, S.; Hanaue, K.-I.; Ohta, K.; Morokuma, K.; Mikami, N.; Fujii, A. Experimental and Theoretical Investigations of Isomerization Reactions of Ionized Acetone and Its Dimer. *Phys. Chem. Chem. Phys.* **2012**, *14*, 712−719.

(5) Matsuda, Y.; Yamada, A.; Hanaue, K.-I.; Mikami, N.; Fujii, A. Catalytic Action of a Single Water Molecule in a Proton-Migration Reaction. *Angew. Chem.* **2010**, *122*, 5018−5021.

(6) Maeda, S.; Matsuda, Y.; Mizutani, S.; Fujii, A.; Ohno, K. Long-Range Migration of a Water Molecule to Catalyze a Tautomerization in Photoionization of the Hydrated Formamide Cluster. *J. Phys. Chem. A* **2010**, *114*, 11896−11899.

(7) Matsuda, Y.; Nakayama, Y.; Mikami, N.; Fujii, A. Isomer-Selective Infrared Spectroscopy of the Cationic Trimethylamine Dimer to Reveal Its Charge Sharing and Enhanced Acidity of the Methyl Groups. *Phys. Chem. Chem. Phys.* **2014**, *16*, 9619−9624.

(8) Yoder, B. L.; Bravaya, K. B.; Bodi, A.; West, A. H. C.; Sztaray, B.; Signorell, R. Barrierless proton transfer across weak CH···O hydrogen bonds in dimethylether dimer. *J. Chem. Phys.* **2015**, *142*, 114303.

(9) Fujii, A.; Fujimaki, E.; Ebata, T.; Mikami, N. Infrared Spectroscopy of CH Stretching Vibrations of Jet-Cooled Alkylbenzene Cations by Using the "Messenger" Technique. *J. Chem. Phys.* **2000**, *112*, 6275−6284.

(10) Douberly, G. E.; Ricks, A. M.; Ticknor, B. W.; Schleyer, P. V. R.; Duncan, M. A. Infrared Spectroscopy of the Tert-Butyl Cation in the Gas Phase. *J. Am. Chem. Soc.* **2007**, *129*, 13782−13783.

(11) Mosley, J. D.; Young, J. W.; Huang, M.; McCoy, A. B.; Duncan, M. A. Infrared Spectroscopy of the Methanol Cation and Its Methylene-Oxonium Isomer. *J. Chem. Phys.* **2015**, *142*, 114301.

(12) Matsuda, Y.; Endo, T.; Mikami, N.; Fujii, A.; Morita, M.; Takahashi, K. The Large Variation in Acidity of Diethylether Cation Induced by Internal Rotation about a Single Covalent Bond. *J. Phys. Chem. A* **2015**, DOI: 10.1021/acs.jpca.5b02604.

(13) Wang, P.; Xing, X.; Baek, S. J.; Ng, C. Y. Rovibrationally Selected and Resolved Pulsed Field Ionization-Photoelectron Study of Ethylene. *J. Phys. Chem. A* **2004**, *108*, 10035−10038.

(14) Hu, Y.; Guan, J.; Bernstein, E. R. Mass-Selected IR-VUV (118 nm) Spectroscopic Studies of Radicals, Aliphatic Molecules, and their Clusters. *Mass Spectrum. Rev.* **2013**, *32*, 484−501.

(15) Matsuda, Y.; Mikami, N.; Fujii, A. Vibrational Spectroscopy of Size-Selected Neutral and Cationic Clusters Combined with Vacuum-Ultraviolet One-Photon Ionization Detection. *Phys. Chem. Chem. Phys.* **2009**, *11*, 1279−1290.

(16) Builth-Williams, J. D.; Bellm, S. M.; Chiari, L.; Thorn, P. A.; Jones, D. B.; Chaluvadi, H.; Madison, D. H.; Ning, C. G.; Lohmann, B.; da Silva, G. B.; et al. A Dynamical (e,2e) Investigation of the Structurally Related Cyclic Ethers Tetrahydrofuran, Tetrahydropyran, and 1,4-Dioxane. *J. Chem. Phys.* **2013**, *139*, 034306.

(17) Giuliani, A.; Limão-Vieira, P.; Duflot, D.; Milosavljevic, A. R.; Marinkovic, B. P.; Hoffmann, S. V.; Mason, N.; Delwiche, J.; Hubin-Franskin, M. J. Electronic States of Neutral and Ionized Tetrahy-

drofuran Studied by VUV Spectroscopy and Ab Initio Calculations. *Eur. Phys. J. D* **2009**, *51*, 97−108.
(18) Ning, C. G.; Huang, Y. R.; Zhang, S. F.; Deng, J. K.; Liu, K.; Luo, Z. H.; Wang, F. Experimental and Theoretical Electron Momentum Spectroscopic Study of the Valence Electronic Structure of Tetrahydrofuran Under Pseudorotation. *J. Phys. Chem. A* **2008**, *112*, 11078−11087.
(19) Dampc, M.; Szymańska, E.; Mielewska, B.; Zubek, M. Ionization and Ionic Fragmentation of Tetrahydrofuran Molecules by Electron Collisions. *J. Phys. B: At., Mol. Opt. Phys.* **2011**, *44*, 055206.
(20) Cadioli, B.; Gallinella, E.; Coulombeau, C. Geometric Structure and Vibrational Spectrum of Tetrahydrofuran. *J. Phys. Chem.* **1993**, *97*, 7844−7856.
(21) Yang, T.; Su, G.; Ning, C.; Deng, J.; Wang, F.; Zhang, S.; Ren, X.; Huang, Y. New Diagnostic of the Most Populated Conformer of Tetrahydrofuran in the Gas Phase. *J. Phys. Chem. A* **2007**, *111*, 4927−4933.
(22) Rayón, V. M.; Sordo, J. A. Pseudorotation Motion in Tetrahydrofuran: An Ab Initio Study. *J. Chem. Phys.* **2005**, *122*, 204303.
(23) Mizuno, K.; Masuda, Y.; Yamamura, T.; Kitamura, J.; Ogata, H.; Bako, I.; Tamai, Y.; Yagasaki, T. Roles of the Ether Oxygen in Hydration of Tetrahydrofuran Studied by IR, NMR, and DFT Calculation Methods. *J. Phys. Chem. B* **2009**, *113*, 906−915.
(24) Eyster, J. M.; Prohofsky, E. W. The Normal Vibrations of Tetrahydrofuran and Its Deuterated Derivatives. *Spectrochim Acta A Mol. Biomol. Spectrosc.* **1974**, *30*, 2041−2046.
(25) Bowron, D. T.; Finney, J. L.; Soper, A. K. The Structure of Liquid Tetrahydrofuran. *J. Am. Chem. Soc.* **2006**, *128*, 5119−5126.
(26) Szmytkowski, C.; Ptasińska-Denga, E. Total Electron-Scattering Cross Section Measurements for Tetrahydropyran, $(CH_2)_5O$, Molecules. *J. Phys. B: At., Mol. Opt. Phys.* **2011**, *44*, 015203.
(27) Stortz, C. A. Conformational Pathways of Simple Six-Membered Rings. *J. Phys. Org. Chem.* **2010**, *23*, 1173−1186.
(28) Naumov, S.; Janovsk, I.; Knolle, W.; Mehnert, R. Radical Cations of Tetrahydropyran and 1,4-Dioxane Revisited: Quantum Chemical Calculations and Low-Temperature EPR Results. *Phys. Chem. Chem. Phys.* **2003**, *5*, 3133−3139.
(29) Cornish, T. J.; Baer, T.; Pedersen, L. G. The n→3s Rydberg Transition of Jet-Cooled Tetrahydropyran, 1, 4-Dioxane, and 1, 4-Dioxane-d8 Studied by 2 + 1 Resonance-Enhanced Multiphoton Ionization. *J. Phys. Chem.* **1989**, *93*, 6064−6069.
(30) Matsuda, Y.; Mori, M.; Hachiya, M.; Fujii, A.; Mikami, N. Infrared Spectroscopy of Size-Selected Neutral Clusters Combined with Vacuum-Ultraviolet-Photoionization Mass Spectrometry. *Chem. Phys. Lett.* **2006**, *422*, 378−381.
(31) Frisch, M. J.; Trucks, G. W.; Schlegel, H. B.; Scuseria, G. E.; Robb, M. A.; Cheeseman, J. R.; Scalmani, G.; Barone, V.; Mennucci, B.; Petersson, G. A.; et al. *Gaussian 09*, revision C 01; Gaussian, Inc., Wallingford CT, 2009. See the Supporting Information for full citation.
(32) Ohno, K.; Maeda, S. A Scaled Hypersphere Search Method for the Topography of Reaction Pathways on the Potential Energy Surface. *Chem. Phys. Lett.* **2004**, *384*, 277−282.
(33) Maeda, S.; Ohno, K. Global Mapping of Equilibrium and Transition Structures on Potential Energy Surfaces by the Scaled Hypersphere Search Method: Applications to ab Initio Surfaces of Formaldehyde and Propyne Molecules. *J. Phys. Chem. A* **2005**, *109*, 5742−5753.
(34) Ohno, K.; Maeda, S. Global Reaction Route Mapping on Potential Energy Surfaces of Formaldehyde, Formic Acid, and Their Metal-Substituted Analogues. *J. Phys. Chem. A* **2006**, *110*, 8933−8941.
(35) Dennington, R.; Keith, T.; Millam, J. *GaussView*, version 5 Semichem Inc.: Shawnee Mission, KS, 2009.
(36) Rauk, A.; Sorensen, T. S.; Maerker, C. Axial and Equatorial 1-Methyl-1-Cyclohexyl Cation Isomers Both Have Chair Conformations but Differ in CC and CH Hyperconjugation Modes. *J. Am. Chem. Soc.* **1996**, *118*, 3761−3762.
(37) Leyssens, T.; Peeters, D. Negative Hyperconjugation in Phosphorus Stabilized Carbanions. *J. Org. Chem.* **2008**, *73*, 2725−2730.
(38) Reed, A. E.; Schleyer, P. v. R. Chemical Bonding in Hypervalent Molecules. The Dominance of Ionic Bonding and Negative Hyperconjugation Over D-Orbital Participation. *J. Am. Chem. Soc.* **1990**, *112*, 1434−1445.
(39) Mo, Y.; Zhang, Y.; Gao, J. A Simple Electrostatic Model for Trisilylamine: Theoretical Examinations of the n→σ^* Negative Hyperconjugation, Pπ→Dπ Bonding, and Stereoelectronic Interaction. *J. Am. Chem. Soc.* **1999**, *121*, 5737−5742.
(40) Rao, V. M.; Kewley, R. Microwave Spectrum and Conformation of Tetrahydropyran. *Can. J. Chem.* **1969**, *47*, 1289−1293.

DOI: 10.1021/acs.jpca.5b03406
J. Phys. Chem. A 2015, 119, 5668−5675